Computational Study of the Structural, Energetical, and Acid-Base Properties of Calix[4]arenes

Peter D. J. Grootenhuis,[†] Peter A. Kollman,[†] Leo C. Groenen,[‡] David N. Reinhoudt,*[,‡] Gerrit J. van Hummel,[§] Franco Ugozzoli,[⊥] and Giovanni D. Andreetti[⊥]

Contribution from the Department of Pharmaceutical Chemistry, University of California, San Francisco, California 94143, the Laboratories of Organic Chemistry and Chemical Physics, University of Twente, P.O. Box 217, 7500 AE Enschede, The Netherlands, and the Institute of Structural Chemistry, University of Parma, Viale delle Scienze, I-43100 Parma, Italy.
Received August 18, 1989

Abstract: In this study some of the properties of calix[4]arenes were assessed by various computational methods. The conformational properties of substituted calixarenes were studied by using molecular mechanics. The preferred conformation of a calix[4]arene depends on the number and the positions of the substituents on the oxygen atoms and is mainly determined by electrostatic interactions. Para substituents have only a minor influence on the relative energies of the conformations. In a number of cases the conformation with the lowest calculated energy is different from the conformation found in solution and in the solid state. The calculated geometries of the conformations found in the X-ray structures and in solution show good agreement with the corresponding X-ray structures. Calculations on calix[4]arene **1i** using different force fields give quite different results, which are mainly caused by differences in the electrostatic energies calculated by these force fields. Some pathways for conformational transitions were studied by molecular dynamics, indicating that the partial cone conformation is a key intermediate. In contrast to previous suggestions, no indications for so-called flip-flop hydrogen bonding were found. The difference in acidity between calixarene **1h** and its acyclic model **2a** was predicted by free energy perturbation methods to be 9-11 pK_a units, in qualitative agreement with experimental data from similar systems. Finally, the energetical and hydrogen-bonding properties of the various calix[4]arene (poly)anions in the gas phase and in aqueous solution were studied by semiempirical molecular orbital and free energy perturbation methods.

Calix[4]arenes **1** are macrocyclic molecules consisting of four phenol units connected via methylene bridges in the ortho positions with respect to the hydroxyl group.[1] They are a class of host compounds that combine a polar and an apolar molecular region, both capable of interacting with a variety of guest molecules. The synthesis and purification of unfunctionalized calixarenes has been optimized very successfully. This renders the calixarenes a very promising class of synthetic host molecules, particularly when selective chemical transformations convert the parent compound into highly organized host molecules, e.g., calixcrowns, calixspherands etc.[2] Such functionalized calixarenes form complexes with metal cations, substituted ammonium ions, and neutral molecules like acetone, toluene, etc.[1]

In this paper we address several questions concerning the properties of calixarenes using computational methods. We have focused on the conformations of various substituted calixarenes. Gutsche[1] has suggested that calixarenes adopt conformations that can be categorized in four classes: the cone, the partial cone, the 1,2-alternate, and the 1,3-alternate conformations (see Figure 1).

Although NMR and X-ray studies have provided quantitative data on these conformations, the relative energetics of the conformations are virtually unknown. First, we have addressed several questions concerning the relative stability of the various conformations using molecular mechanics (MM) calculations,[3,4] e.g., the dominating forces that control the conformation, the effect of substitution of the hydroxyl groups, and the effect of the para substituents on the conformation. The results of the calculations are compared with the data obtained from ^{1}H NMR and X-ray studies. Subsequently, we have evaluated the results of various molecular mechanics models [AMBER, MM2P(85), the AMBER and MM2 force fields implemented in MACROMODEL, and CHARMm in the QUANTA program] and a semiempirical method (AM1) by comparing the structures and corresponding energies calculated for one particular calixarene. Second, molecular dynamics (MD) simulations have been used to evaluate possible pathways for conformational transitions. Gutsche has suggested[1] that the type of circular hydrogen bonding known as flip-flop hydrogen bonding[5] could very well be present in calixarenes. Since MD simulations were applied successfully in order to investigate hydrogen-bonding patterns in cyclodextrins,[6] we have analyzed the calixarenes in

Chart I

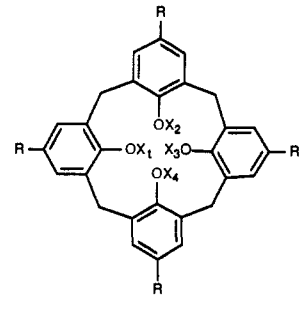

	X_1	X_2	X_3	X_4	R
1a	H	H	H	H	*t*-Bu
1b	Me	H	H	H	*t*-Bu
1c	Me	H	Me	H	*t*-Bu
1d	Me	Me	H	H	*t*-Bu
1e	Me	Me	Me	H	*t*-Bu
1f	Me	Me	Me	Me	*t*-Bu
1g	Me	H	Me	H	H
1h	H	H	H	H	Me
1i	Me	Me	Me	Me	Me

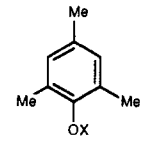

	X
2a	H
2b	Me

[†] University of California.
[‡] Laboratory of Organic Chemistry, University of Twente.
[§] Laboratory of Chemical Physics, University of Twente.
[⊥] University of Parma.

(1) Gutsche, C. D. *Prog. Macrocyclic Chem.* **1987**, *3*, 93-165.
(2) (a) Reinhoudt, D. N.; Dijkstra, P. J.; in't Veld, P. J. A.; Bugge, K.-E.; Harkema, S.; Ungaro, R.; Ghidini, E. *J. Am. Chem. Soc.* **1987**, *109*, 4761-4762. (b) Dijkstra, P. J.; Brunink, J. A. J.; Bugge, K.-E.; Reinhoudt, D. N.; Harkema, S.; Ungaro, R.; Ghidini, E. *J. Am. Chem. Soc.* **1989**, *111*, 7567-7575.
(3) Burkert, U.; Allinger, N. L. *Molecular Mechanics*; ACS Monograph 177; American Chemical Society: Washington, DC, 1982.
(4) Clark, T. *A Handbook of Computational Chemistry*; John Wiley and Sons: New York, 1985.
(5) (a) Sänger, W. *Nature* **1979**, *279*, 343-344. (b) Sänger, W.; Betzel, C.; Hingerty, B.; Brown, G. M. *Nature* **1982**, *296*, 581-583. (c) Sänger, W.; Betzel, C.; Hingerty, B.; Brown, G. M. *Angew. Chem., Int. Ed. Engl.* **1983**, *22*, 883-884.

0002-7863/90/1512-4165$02.50/0 © 1990 American Chemical Society

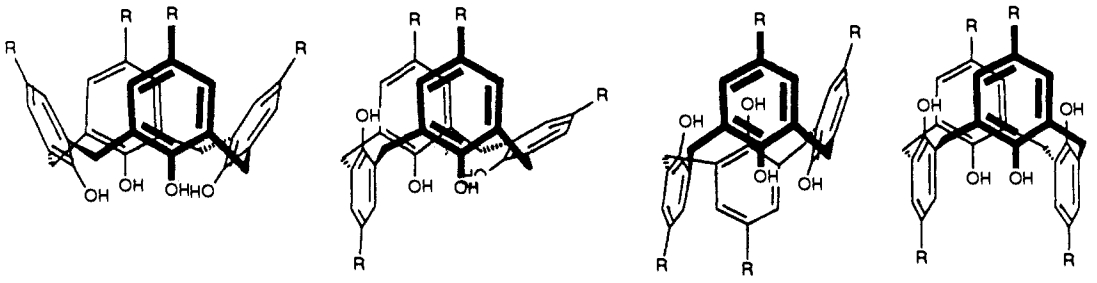

cone partial cone 1,2-alternate 1,3-alternate

Figure 1. Schematic drawing of the conformations of calix[4]arenes.

a similar fashion. Third, we have studied the proton dissociation equilibria of calixarenes. Preliminary reports on the acidity of water-soluble calixarenes, suggest that calixarenes possess very intriguing acid–base properties. Shinkai and co-workers have shown that calixarenes are much more acidic than the corresponding open-chain model compounds.[7] By use of a free energy perturbation (FEP) approach the difference in pK_a between calixarene **1h** and its open-chain model compound **2a** has been calculated. In addition, the relative acidities for removing a second, third, and fourth proton have been studied. Hitherto, in the field of synthetic host–guest chemistry, FEP methods have only been applied to studying differences in binding free energies of host–guest complexes by perturbing one guest into another.[8] We are only aware of one example where FEP methods were used for calculating differences in acidities of compounds, i.e., a study by Jorgensen and co-workers, who calculated the relative acidities of ethane and acetonitrile in water.[9] Finally, the charge delocalization and hydrogen bonding in the (poly)anionic forms of **1h** have been studied by using semiempirical molecular orbital methods.

To our knowledge, the work presented here represents the first general computational study of the properties of calix[4]arenes.

Methods and Computational Details

In this study several programs have been used for calculations on calix[4]arenes. The conformations of calix[4]arenes with different substituents on the oxygen atoms and on the para positions were studied with the program MACROMODEL version 1.5.[10] The effect of different force fields on the energies of the conformations of one particular calix[4]arene was studied with the programs MACROMODEL (AMBER and MM2 force fields), MM2P(85),[11] AMBER version 3.0,[12] and QUANTA 2.1A (CHARMm).[13] For the semiempirical calculations AMPAC (AM1) was used.[14] The molecular dynamics and free energy perturbation calculations and the calculation of relative acidities were performed with the program AMBER.

Table I. Additional Parameters for Calculations on Calix[4]arenes with the AMBER 3.0 Program

bond	K_r, kcal mol^{-1} Å^{-2}	r_{eq}, Å
C–OS	425.0	1.338
CA–OS	300.0	1.40
angle	K_θ, kcal mol^{-1} radian^{-2}	θ_{eq}, deg
CA–OS–C	55.0	109.9
CA–OS–CT	46.5	113.0
OS–C–O	80.0	122.0
OS–C–CT	63.0	107.1
CA–CT–CA	70.0	120.0
C–CA–CT	70.0	120.0
dihedral	$V_n/2$, kcal mol^{-1}	γ, deg n
X–CA–OS–X	2.0	180.0 2
improper dihedral	V_n, kcal mol^{-1}	γ, deg n
CA–CA–CA–CA	20.0	180.0 2
CA–C–CA–CA	20.0	180.0 2

Molecular Mechanics Calculations. The calculations on differently substituted calix[4]arenes were performed with the all-atom AMBER force field as it is implemented in the program MACROMODEL. This force field was chosen because it includes a potential for the fine tuning of hydrogen bonds. This force field differs from the original AMBER force field[15] in that generalized parameters have been added to allow modeling on many types of molecules, besides the peptides and DNA molecules for which the force field was developed. The force field was used without modification of any of the parameters. This means that electrostatic energies were calculated by using point charges derived from bond dipole moments given in the standard AMBER parameter list of MACROMODEL.[10] A constant dielectric with $\epsilon = 1.0$ was used. The 1–4 van der Waals and 1–4 electrostatic energies were scaled down by a factor of 0.5. The cutoff distances for the van der Waals and electrostatic interactions were set to a value of 100 Å to allow all interactions to be taken into account.

Starting geometries were manually input by use of the ORGANIC INPUT mode of the program. From the cone conformation the other three main conformations, the partial cone, the 1,2-alternate and the 1,3-alternate, were easily derived by adjustment of the dihedral angles around the bonds of the phenyl groups to the methylene carbon atoms. We tried a number of different dihedral angles for the starting structures, but always ended up with one of the four main conformations after energy minimization. Therefore, we did not undertake an extensive search for possible other ring conformations by systematically varying all dihedral angles in the ring. For each main conformation the positions of the OR groups relative to the aromatic moiety were systematically varied to find the lowest energy conformation. Each *tert*-butyl group can

(6) (a) Köhler, J. E. H.; Sänger, W.; van Gunsteren, W. F. *Eur. Biophys. J.* **1987**, *15*, 197–210. (b) Köhler, J. E. H.; Sänger, W.; van Gunsteren, W. F. *Eur. Biophys. J.* **1987**, *15*, 211–224. (c) Köhler, J. E. H.; Sänger, W.; van Gunsteren, W. F. *J. Biomol. Struct. Dyn.* **1988**, *6*, 181–198. (d) Köhler, J. E. H.; Sänger, W.; van Gunsteren, W. F. *J. Mol. Biol.* **1988**, *203*, 241–250. (e) Köhler, J. E. H.; Sänger, W.; van Gunsteren, W. F. *Eur. Biophys. J.* **1988**, *16*, 153–168.

(7) Shinkai, S.; Araki, K.; Koreishi, H.; Tsubaki, T.; Manabe, O. *Chem. Lett.* **1986**, 1351–1354.

(8) (a) Lybrand, T. P.; McCammon, J. A.; Wipff, G. *Proc. Natl. Acad. Sci. U.S.A.* **1986**, *83*, 833–835. (b) Grootenhuis, P. D. J.; Kollman, P. A. *J. Am. Chem. Soc.* **1989**, *111*, 2152–2158. (c) van Eerden, J.; Harkema, S.; Feil, D. *J. Phys. Chem.* **1988**, *92*, 5076–5079. (d) Mazor, M. H.; McCammon, J. A.; Lybrand, T. P. *J. Am. Chem. Soc.* **1989**, *111*, 55–56. (e) Jorgensen, W. L.; Boudon, S.; Nguyen, T. B. *J. Am. Chem. Soc.* **1989**, *111*, 755–757. (f) Grootenhuis, P. D. J.; Kollman, P. A. *J. Am. Chem. Soc.* **1989**, *111*, 4046–4051.

(9) Jorgensen, W. L.; Briggs, J. M.; Gao, J. *J. Am. Chem. Soc.* **1987**, *109*, 6857–6858.

(10) Still, W. C. MACROMODEL version 1.5, Department of Chemistry, Columbia University, New York, 1987.

(11) MM2P(85) is an improved and enlarged version of MMP2; see: Sprague, J. T.; Tai, J. C.; Yuh, Y.; Allinger, N. L. *J. Comput. Chem.* **1987**, *8*, 581–603, and references cited.

(12) Singh, U. C.; Weiner, P. K.; Caldwell, J.; Kollman, P. A. AMBER 3.0, University of California—San Francisco, 1987.

(13) QUANTA 2.1A, released August 1989, purchased from Polygen Corp., Waltham, MA.

(14) AMPAC, QCPE program No. 506, Dewar Research Group, University of Texas, Austin and Stewart, J. J. P. Seiler Research Labs, U.S. Air Force Academy, Colorado Springs, CO.

(15) (a) Weiner, P. K.; Kollman, P. A. *J. Comput. Chem.* **1981**, *2*, 287–303. (b) Weiner, S. J.; Kollman, P. A.; Case, D. A.; Singh, U. C.; Ghio, C.; Alagona, G.; Profeta, S., Jr.; Weiner, P. *J. Am. Chem. Soc.* **1984**, *106*, 765–784. (c) Weiner, S. J.; Kollman, P. A.; Nguyen, D. T.; Case, D. A. *J. Comput. Chem.* **1986**, *7*, 230–252.

Chart II

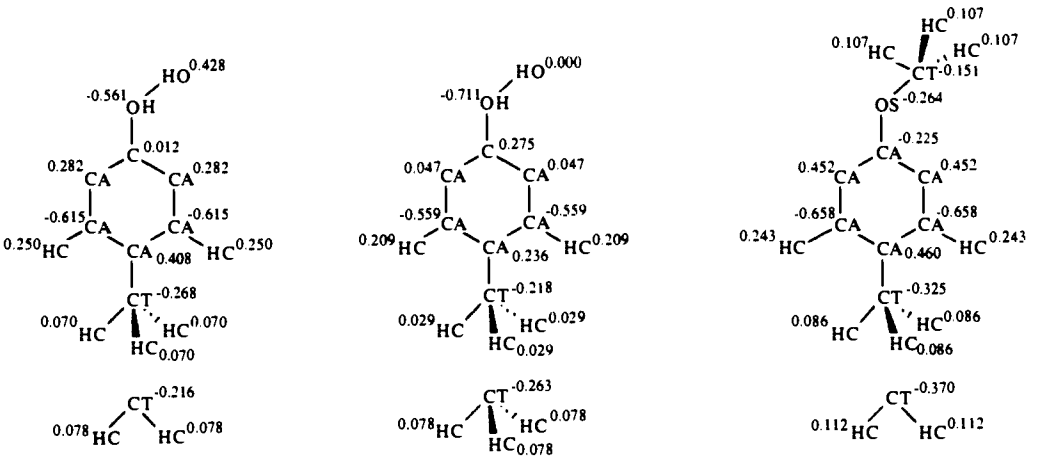

assume two positions with different energies, depending also on the positions of the other *tert*-butyl groups. The energy differences were very small (typically <0.1 kcal mol^{-1}), so that no attempt was made to find in each case the most favorable position of the four *tert*-butyl groups. All reported conformations were minimized until the root mean square (rms) of the first derivative of the energy was less than 0.0002 kcal mol^{-1} Å^{-1} and were checked to be minima on the potential energy surface by computing the eigenvalues of the second-derivative matrix, of which six should be zero and all others positive.

The comparison of the force fields was performed for the tetramethyl ether of *p*-methylcalix[4]arene **1i**. This compound was chosen because it has no hydroxyl groups (to avoid the problems of hydrogen bonds) and it has methyl groups instead of *tert*-butyl groups at the para positions, which makes the calculations easier and faster. The molecule is of course still a good representative of a calix[4]arene. Starting geometries for the four main conformations were taken from the minimized AMBER (MACROMODEL) structures of the *p-tert*-butyl derivative **1f**. The AMBER (MACROMODEL) energies were calculated in the same way as described above. The MM2 (MACROMODEL) energies were calculated with the unadjusted force field as it is implemented in MACROMODEL. The parameters in this force field are derived from the 1985 version of MM2,[11] but in MACROMODEL the electrostatic energies are calculated with atomic point charges instead of bond dipole moments as in the original MM2 program. The MM2 energies of the four conformations were also calculated with the original program MM2P(85),[11] which was used without any modification.

The CHARMm force field as present in version 2.1A of QUANTA[13] was found not to reproduce well the position of the OMe group relative to the benzene moiety. Reduction of the force constant for the X-C6R-OE-X dihedral angle constant from 3.0 to 1.0 kcal mol^{-1} led to satisfying geometries. Also here, as in MACROMODEL, the cutoff distance for nonbonded interactions was set to 100 Å and a constant dielectric $\epsilon = 1.0$ was used.

In the calculations in which the AMBER package[12,15] was used, the all-atom force field was used in all cases. Most of the force field parameters have been previously published.[15c] A list of all additional parameters used in the present study is given in Table I.

Electrostatic point charges for all studied molecules were obtained by optimizing the geometries of several acyclic model systems, i.e., anisole, 2,4,6-trimethylphenol (**2a**), the corresponding monoanion, and methyl ether **2b**, by the semiempirical AM1 method.[16] For **2b** the conformation was taken in which the substituent at the oxygen is in a position out of the plane through the aromatic moiety. After the geometry optimizations a single-point ab initio calculation was carried out with a 6-31G* basis set. Finally, the charges were fitted to the thus obtained electrostatic potential[17] at the van der Waals surface of the molecules by using GAUSSIAN 80 UCSF.[18] All partial charges and atom types are given in Chart II.

The starting geometries for the molecular mechanical calculations on the calixarenes were model built by using the molecular graphics software MIDAS.[19] The geometries of the complexes were optimized with AMBER until the rms energy gradient was less than 0.001 kcal mol^{-1} Å^{-1}. Throughout all calculations a constant dielectric with ϵ equal to 1.0 and a scale factor of 0.5 for the 1-4 VDW and 1-4 electrostatic interactions was used (SCNB = SCEE = 2.0).[15b,c] There was no cutoff for the nonbonded interactions in the MM calculations.

Semiempirical Calculations. In all semiempirical calculations the AM1 Hamiltonian[16] in the AMPAC program[14] was used. Geometries were fully optimized without applying any constraints. As starting geometries for the calculations on calixarenes and its acyclic model, the corresponding AMBER 3.0 minimized structures were used.

Molecular Dynamics. Three 50-ps MD runs were performed starting with one isolated molecule **1h** in the cone formation, equilibrated for 10 ps at 300 K. The three runs were carried out at temperatures of 300, 600, and 800 K. The same cutoff, scaling factors, etc. were used as in the molecular mechanics calculations. No SHAKE[20] was applied, meaning that no constraints were applied to the equilibrium bond lengths. The coordinates were saved every 0.025 ps for further analysis. One 50-ps MD run was carried out for **1h** surrounded by a spherical droplet of 236 water molecules at $T = 300$ K. The coordinates were saved every 0.1 ps. More details are given under Free Energy Perturbation Calculations.

Free Energy Perturbation Calculations. We used FEP theory[21] in order to estimate the relative acidities of calixarene **1h** and its acyclic analogue 2,4,6-trimethylphenol (**2a**). In the perturbation calculations the free energy difference is calculated between two states of a system, A and B, by using results from statistical mechanics.[21] In the window growth approach, a variable λ is introduced in the potential energy function V, defined in such a way that at $\lambda = 0$, $V = V_A$, and at $\lambda = 1$, $V = V_B$. The following equation can be derived:

$$\Delta G = G_B - G_A = \sum_{i=1}^{N} -RT \ln \langle e^{-V(r,\lambda_i)-V(r,\lambda_{i-1})/RT} \rangle_{\lambda_{i-1}} \qquad (1)$$

in which r indicates the coordinate vector, $\langle\rangle_{\lambda_{i-1}}$ denotes that the ensemble average is calculated, R is the molar gas constant, and T is the temperature. In this study the two states correspond to the nth and $n+1$th deprotonated forms of the calixarene **1h** ($n = 0-3$, $m = 4-n$) or its acyclic model **2a** ($n = 0$, $m = 1$).

$$H_mA^{n-}{}_{aq} \xrightarrow{\Delta G_{pert}} H_{m-1}A^{(n+1)-}{}_{aq} \qquad (2)$$

The AMBER-minimized conformations of the molecules were encapsulated in droplets of ±240 TIP3P water molecules[22] within 8-Å distance

(16) Dewar, M. J. S.; Zoebisch, E. G.; Healy, E. F.; Stewart, J. J. P. *J. Am. Chem. Soc.* **1985**, *107*, 3902–3909.
(17) Singh, U. C.; Kollman, P. A. *J. Comput. Chem.* **1984**, *5*, 129–145.
(18) Singh, U. C.; Kollman, P. A. GAUSSIAN 80 UCSF. *Quantum Chem. Exchange Program Bull.* **1982**, *2*, 17.
(19) Ferrin, T. E.; Huang, C. C.; Jarvis, L. E.; Langridge, R. *J. Mol. Graphics* **1988**, *6*, 13–27.
(20) van Gunsteren, W. F.; Berendsen, H. J. C. *Mol. Phys.* **1977**, *34*, 1311–1327.
(21) (a) Bash, P. A.; Singh, U. C.; Langridge, R.; Kollman, P. A. *Science* **1987**, *236*, 564–568. (b) Singh, U. C.; Brown, F. K.; Bash, P. A.; Kollman, P. A. *J. Am. Chem. Soc.* **1987**, *109*, 1607–1614. (c) McCammon, J. A. *Science* **1987**, *238*, 486–491. (d) van Gunsteren, W. F. *Protein Eng.* **1988**, *2*, 5–13. (e) *Computer Simulations of Biomolecular Systems*; van Gunsteren, W. F., Weiner, P. K., Eds.; ESCOM: Leiden, 1989. (f) Allen, M. P.; Tildesley, D. J. *Computer Simulations of Liquids*; Clarendon Press: Oxford, 1987. (g) Brooks, C. L.; Karplus, M.; Pettitt, B. M. In *Proteins, A Theoretical Perspective of Dynamics, Structure, and Thermodynamics*; Prigogine, I., Rice, S. A., Eds.; Advances in Chemical Physics 71; John Wiley & Sons: New York, 1988. (h) Mezei, M.; Beveridge, D. L. *Ann. N.Y. Acad. Sci.* **1986**, *482*, 1–23. (i) Jorgensen, W. L. *Acc. Chem. Res.* **1989**, *22*, 184–189. (j) Pearlman, D. A.; Kollman, P. A. *J. Chem. Phys.* **1989**, *90*, 2460–2470.
(22) Jorgensen, W. L.; Chandrasekhar, J.; Madura, J.; Impey, R. W.; Klein, M. L. *J. Chem. Phys.* **1983**, *79*, 926–935.

of the center of mass of the solute. Small harmonic constraints of, respectively, 2.0 and 0.6 kcal mol^{-1} were applied in order to keep the compound in the center of the droplet and to prevent the solvent molecules from "evaporating" during the calculations. The residue-based cutoff for the nonbonded interactions was set to 8 Å after verifying that this was enough to evaluate all intramolecular interactions due to changes in the partial atomic charges upon the perturbation.

MD was used in order to generate ensembles along the reaction pathway. Starting geometries for the MD simulations were the energy-minimized structures from the MM studies with AMBER. Before every MD run the structures were equilibrated at 300 K for 10 ps. This period appeared to be sufficient to reach a plateau value for the potential energy of the system. The SHAKE procedure was applied to constrain all covalent bonds involving a hydrogen atom to their equilibrium lengths.[20] The temperature was maintained at 300 K by velocity scaling using a relaxation time of 0.1 ps. The translational and rotational motion around the center of mass of the system was removed every 500 steps. Each perturbation calculation consisted of 21 windows ($\Delta\lambda = 0.05$). At each window 500 steps of equilibration and 500 data collection steps were performed. Since the time step was 0.001 ps, the total time for one perturbation run amounts to 21 ps. All runs were performed forward (λ: $1 \rightarrow 0$) and backward (λ: $0 \rightarrow 1$). A number of test runs was performed in order to make sure that the relevant parameters such as the time step (0.001 ps), the length of the trajectory (21 ps), and the number of windows (21) had satisfying values and the free energies calculated were not artifacts of the parameter choice. Since the ensembles were generated at constant temperature (300 K) and pressure (0 atm), the energies calculated may be regarded as Gibbs free energies. The time for a single perturbation run in which 21 ps of molecular dynamics was evaluated was approximately 10–15 CPU h on a Convex C1 running under the Unix operating system.

Calculation of the Relative Acidities. The dissociation equilibria of two species HA and HB in this study are given by

$$HA_{aq} \overset{K_a(HA)}{\rightleftharpoons} A^-_{aq} + H^+_{aq}$$

and

$$HB_{aq} \overset{K_a(HB)}{\rightleftharpoons} B^-_{aq} + H^+_{aq}$$

However, since we are only interested in the *difference* of the acidities of HA and HB, i.e., $pK_a(HB) - pK_a(HA)$, we studied a system that is computationally easier to evaluate, in which the common species, viz. H^+_{aq}, is eliminated.

This means that we can calculate a ΔpK_a value according to eq 3.

$$K_a'(HA) = \frac{[A^-]_{aq}}{[HA]_{aq}}$$

$$K_a'(HB) = \frac{[B^-]_{aq}}{[HB]_{aq}}$$

$$\Delta pK_a = pK_a(HB) - pK_a(HA) = \log \frac{K_a(HA)}{K_a(HB)} = \log \frac{K_a'(HA)}{K_a'(HB)} \quad (3)$$

The hydration of the species in the simulations was mimicked by dividing it into two parts. The first solvation shells were simulated by encapsulating the species in a droplet with a radius of 8 Å of water molecules (vide supra), which were included in the MD calculations. The nonbonded cutoff was 8 Å. Subsequently, the Born formula was applied for estimating the hydration free energy of this ion with a formal radius of 8 Å:

$$\Delta G_{hydr} = -\frac{N_A z^2 e^2}{8\pi\epsilon_0 r}\left(1 - \frac{1}{\epsilon}\right) \quad (4)$$

in which N_A is Avogadro's number (6.022×10^{23} mol^{-1}), z the charge of the ion in units of e, the elementary charge (1.6022×10^{-19} C), r the ionic radius in m, ϵ_0 the permittivity of a vacuum (8.8542×10^{-12} F m^{-1}), and ϵ the relative dielectric constant of the fluid (for water, 78.3). It is essential to take this reaction field correction into account when comparing two species with different charges, which was the case for our polydeprotonation studies on calixarene **1h**. By substitution of the various constants with the appropriate values, eq 4 can be rewritten in the following form:

$$\Delta G_{hydr} = -164z^2/r \quad (5)$$

with ΔG_{hydr} in kcal mol^{-1}, r the radius of the ion in Å, and z the charge of the ion. For the nth deprotonation (eq 2), the reaction field correction (in kcal mol^{-1}) for the partly solvated ions with a formal radius of 8 Å is given by eq 6.

$$\Delta G_{corr} = -20.5(2n + 1) \quad (6)$$

The total free energy difference ΔG_{total} is then calculated as the sum of ΔG_{pert} and ΔG_{corr}.

$$\Delta G_{total} = \Delta G_{pert} + \Delta G_{corr} \quad (7)$$

Using a molecular mechanical potential energy function, it is not possible to account for the energy required to break the O–H bond. Therefore, we have to assume that this quantity is the same for equivalent species, and it drops out of the equations when one is only interested in the difference in free energies of those species. The difference in ΔG_{total} (expressed in kcal mol^{-1}) at 300 K for two compounds is directly related to their difference in the pK_a values according to

$$\Delta\Delta G_{total} = 1.4\Delta pK_a \quad (8)$$

X-ray Diffraction. X-ray measurements of the three compounds **1c**, **1e**, and **1f** were performed on a Siemens A.E.D. single-crystal diffractometer, using Ni-filtered Cu Kα ($\lambda = 1.541\,78$ Å), on line to a General Automation microcomputer. Reflections were measured in the $\omega/2\theta$ scanning mode (scan speed, 3–12 deg min^{-1}; scan width, $(\theta - 0.5) - [\theta + (0.6 + \Delta\theta)]$; $\Delta\theta = (\lambda\alpha_2 - \lambda\alpha_1)/\tan\theta$), with θ ranging from 2.5 to 70° (compound **1c**, 3–70°). The most relevant data collection parameters are reported in Table II.

Measured intensities were corrected for Lorentz and polarization effects. No corrections were applied for the absorption effects. The structures were solved by direct methods and refined with unit weights by block full-matrix least-squares methods using the SHELX[23] package of crystallographic computer programs. All H atoms were calculated with the geometrical constraint C–H 1.08 Å, and the methyl groups were refined as rigid bodies.

The refinement of compound **1c** was carried out in two blocks of full-matrix least squares of 269 parameters. Parameters refined were the overall scaling factor, positional parameters, anisotropic thermal parameters for all non-hydrogen atoms, isotropic thermal parameters for the aromatic hydrogens, and the common thermal parameters for the rigid bodies.

The refinement of compound **1e** was performed in four blocks of full-matrix least squares of 158, 131, 131, and 131 parameters, respectively. Parameters refined were the overall scaling factor, positional parameters, anisotropic thermal parameters for all non-hydrogen atoms, and isotropic thermal parameters for hydrogens.

The structure of compound **1f** consists of two independent molecules in the asymmetric unit, which show only negligible differences. The refinement was carried out in two blocks of full-matrix least squares of 209 parameters. Parameters refined were the overall scaling factor, positional parameters, and isotropic thermal parameters for all non-hydrogen atoms.

Scattering factors were taken from the literature.[24] Geometrical calculations were performed with PARST.[25] All the calculations were performed on a GOULD 32/70 of Centro di Strutturistica Diffrattometrica del CNR, Parma, Italy.

X-ray diffraction data for **1g** were collected on a Philips PW1100 single-crystal diffractometer, using Mo Kα radiation monochromated by a graphite crystal ($\lambda = 0.710\,69$ Å). Reflections were measured in the $\omega/2\theta$ scanning mode (maximum scan speed, 0.05 s^{-1}; scan width, 1.0°; $2 < \theta < 25°$). The maximum variation in 3 standard reflections was 1.8%. Relevant data collection parameters are reported in Table II.

The structure was solved by direct methods[26] and was refined by the full-matrix least-squares procedure.[27] Hydrogen atoms were located by difference Fourier maps. The methoxy and hydroxyl hydrogen atoms could not be found in either of the two independent molecules in the asymmetric unit. The refined parameters included the scaling factor, positional parameters, anisotropic thermal parameters for non-hydrogen atoms, and isotropic thermal parameters for hydrogen atoms. The weight of each reflection was calculated as $w = 1/\sigma^2(F)$, $\sigma^2(F) = \sigma^2(I) + (pF^2)^2$, $p = 0.04$. Scattering factors for non-hydrogen atoms were taken from the literature;[24] for hydrogen atoms the scattering factors of Stewart et

(23) Sheldrick, G. M. *SHELX. Computer programs for crystal structure determinations*. University of Cambridge, UK, 1980.
(24) *International Tables for X-ray Crystallography*; Kynoch Press: Birmingham, England, 1974; Vol. IV, pp 72–98.
(25) Nardelli, M. *Comput. Chem.* **1983**, 7, 95–98.
(26) Germain, G.; Main, P.; Woolfson, M. M. *Acta Crystallogr., Sect. A* **1971**, *27*, 368–376.
(27) Busing, W. R.; Martin, K. O.; Levy, H. A. ORFLS. Report ORNL-TM-305; Oak Ridge National Laboratory, Oak Ridge, TN, 1962.

Table II. Experimental Data for the X-ray Diffraction Studies on Compounds **1c**, **1e**, **1f**, and **1g**

	1c	**1e**	**1f**	**1g**
crystal habit and color	colorless prism	colorless elongated prism	colorless prism	colorless prism
crystal dimensions, mm	0.2 × 0.3 × 0.4	0.2 × 0.2 × 0.5	0.3 × 0.3 × 0.4	0.3 × 0.3 × 0.3
formula	$C_{46}H_{60}O_4$	$C_{47}H_{62}O_4$	$C_{48}H_{64}O_4$	$C_{30}H_{28}O_4$
fw	676.98	691.00	705.03	452.55
crystal system	monoclinic	monoclinic	monoclinic	monoclinic
space group	$P2_1/n$	$P2_1/n$	$P2_1/a$	$P2_1/c$
T, K	295	295	295	298
cell parameters[a]				
a, Å	19.319 (2)	20.739 (3)	28.511 (4)	19.727 (1)
b, Å	16.168 (3)	20.650 (3)	19.872 (3)	12.073 (1)
c, Å	13.273 (3)	10.316 (2)	16.880 (2)	20.448 (1)
β, deg	91.27 (2)	80.25 (2)	104.08 (2)	100.20 (1)
V, Å^3	4145 (1)	4354 (1)	9276 (2)	4793 (1)
Z	4	4	8	8
D_{calcd}, g cm^{-3}	1.085	1.054	1.01	1.254
μ, cm^{-1}	4.9	4.7	4.5	0.77
no. of reflections measd	$\pm h,k,l$	$\pm h,k,l$	$\pm h,k,l$	$\pm h,k,l$
no. of unique total data	7880	6600	16835	8442
no. of unique obsd data	4872 ($I \geq 2\sigma(I)$)	3108 ($I \geq 2(\sigma(I))$	5420 ($I \geq 2\sigma(I)$)	3614 ($I > \sigma(I)$)
agreement between equivalent obsd data	0.05	0.06	0.09	*b*
no. of variables	538	551	418	773
R	0.064	0.067	0.16	0.075
R_w	0.064	0.067	0.16	0.072
$(\Delta/\sigma)_{max}$	0.07	0.06	0.08	0.85[c]

[a] Unit cell parameters were obtained by least-squares analysis of the setting angles of 25–30 reflections. [b] No symmetry-related reflections were measured. [c] Largest shift for non-hydrogen thermal parameter.

Table III. Results of Molecular Mechanics Calculations on Different Conformations of the Methyl Ethers of *p-tert*-Butylcalix[4]arene (**1a–f**) and of Calix[4]arene, Dimethyl Ether **1g**[a,b]

compd	conformation	E_{total}	E_{str}	E_{bend}	E_{tor}	$E_{bnd,total}$	E_{VDW}	E_{elec}	E_{Hbnd}
1a	cone	−2.0	2.2	5.1	2.1	9.4	11.6	−23.0	−1.5
	partial cone	5.7	2.2	4.9	2.1	9.1	10.3	−13.8	−0.9
	1,2-alternate	9.3	2.3	7.5	1.3	11.1	11.9	−13.6	−1.0
	1,3-alternate	10.6	2.2	4.3	1.6	8.1	7.7	−5.2	0
1b	cone	9.4	2.2	5.3	5.5	13.0	10.3	−13.8	−1.3
	partial cone	10.1	2.2	5.2	5.8	13.1	9.3	−12.4	−0.9
	1,2-alternate	14.8	2.3	7.4	4.9	14.8	10.8	−10.8	−1.0
	1,3-alternate	14.8	2.2	4.5	4.9	11.5	7.0	−3.8	0
1c	cone	19.4	2.1	5.6	8.2	15.9	9.1	−5.5	−1.1
	partial cone	19.3	2.1	5.2	10.8	18.1	8.0	−6.8	−1.0
	1,2-alternate	20.1	2.3	7.2	9.4	18.9	9.5	−8.3	−1.0
	1,3-alternate	19.1	2.2	4.7	8.4	15.3	6.4	−2.6	0
1d	cone	19.0	2.2	5.5	9.9	17.6	8.8	−7.4	−1.0
	partial cone	16.2	2.2	5.3	9.3	16.8	8.7	−9.3	−1.0
	1,2-alternate	21.4	2.3	7.2	9.2	18.7	9.9	−7.2	−1.0
	1,3-alternate	19.1	2.2	4.7	8.6	15.5	6.2	−2.7	0
1e	cone	26.7	2.2	5.6	12.5	20.4	7.6	−1.3	−0.5
	partial cone	23.9	2.2	5.2	12.3	19.7	7.2	−3.0	−0.5
	1,2-alternate	27.0	2.3	6.7	12.5	21.5	9.0	−3.5	−0.5
	1,3-alternate	23.2	2.2	4.9	12.3	19.4	5.5	−1.7	0
1f	cone	33.6	2.3	5.7	16.2	24.2	6.5	+2.9	0
	partial cone	29.0	2.3	5.3	16.0	23.6	5.7	−0.2	0
	1,2-alternate	33.9	2.4	6.4	15.4	24.1	8.7	+1.0	0
	1,3-alternate	27.2	2.3	5.1	15.9	23.2	4.9	−0.9	0
1g	cone	11.2	1.0	1.5	7.8	10.3	3.4	−1.4	−1.1
	partial cone	11.3	1.0	1.3	10.2	12.5	2.5	−2.7	−1.0
	1,2-alternate	11.7	1.2	3.4	8.8	13.4	3.5	−4.1	−1.0
	1,3-alternate	11.6	1.0	0.7	8.0	9.6	1.4	+0.5	0

[a] All energies are in kcal mol^{-1}. [b] Abbreviations used: $E_{total} = E_{bnd,total} + E_{VDW} + E_{elec} + E_{Hbnd}$; $E_{bnd,total} = E_{str} + E_{bend} + E_{tor}$; E_{bnd} denotes the sum of all bonded interactions; E_{VDW} denotes the van der Waals energy; E_{elec} denotes the electrostatic energy; E_{Hbnd} denotes the hydrogen bonding energy; E_{str} denotes the energy associated with bond stretching; E_{bend} denotes the energy associated with angle bending; E_{tor} denotes the energy associated with normal and improper torsional strain.

al. were used.[28] Two hydrogen atoms of two different methylene groups were badly characterized.

Results

Conformational Analysis of Calix[4]arenes. The effects of substituents on the oxygen atoms on the preferred conformation of a calix[4]arene were studied by using the methyl ethers of *p-tert*-butylcalix[4]arene (**1a–f**) as model compounds. The methyl ethers have been chosen because they are flexible and can in principle assume every possible conformation.[29] The *p-tert*-butyl derivatives have been studied extensively by both ^{1}H NMR and X-ray crystallographic methods. The results of the molecular mechanics calculations on the cone, partial cone, 1,2-alternate, and 1,3-alternate conformations of *p-tert*-butylcalix[4]arene and its methyl ethers are summarized in Table III. For most of the compounds more than one representative of each conformation

(28) Stewart, R. F.; Davidson, E. R.; Simpson, W. T. *J. Chem. Phys.* **1965**, *42*, 3175–3187.

(29) Gutsche, C. D.; Dhawan, B.; Levine, J. A.; No, K. H.; Bauer, L. J. *Tetrahedron* **1983**, *39*, 409–426.

can be distinguished, because of the asymmetry introduced in the molecule when one or more hydroxyl groups are replaced by methoxy groups. The orientation of the hydroxyl and methoxy groups can also vary. For each compound only the representative of each of the four conformations with the lowest energy is listed.

For calixarene **1a** the calculations predict a cone conformation with a 4-fold axis of symmetry to be of lowest energy. This is in full agreement with results from dynamic ^{1}H NMR studies[30] and NOE experiments at lower temperatures[31] on phenolic calix[4]arenes. X-ray studies of *p-tert*-octylcalix[4]arene and some clathrates of **1a** also show the calixarene moiety to be present in a cone conformation with C_{4v} symmetry.[32] The geometry of the calixarene moiety can best be characterized by the dihedral angles between the mean plane of each of the phenyl rings and the mean plane of the four methylene groups. These are all 58.1° in the calculated cone conformation of **1a**. In the toluene complex of **1a** these dihedral angles are all 57°.[32a] Furthermore, the distances between oxygen atoms on neighboring phenyl rings give some information about the hydrogen bonding between the phenol groups. These are 2.73 Å in the calculated cone, which compares reasonably well with the experimental value in the toluene complex, 2.67 Å.

The calculated energy differences between the cone conformation and the other conformations originate from the very favorable electrostatic interactions in the cone conformation due to optimal hydrogen bonding. It must be noted here that most of the energy associated with hydrogen bonding is found in the E_{elec} term. The E_{Hbnd} term was introduced to the AMBER force field in order to fine tune the geometry of hydrogen bonds, but it hardly contributes to the energy associated with hydrogen bonding.

When one of the hydroxyl groups is substituted by a methoxy group, the cone conformation remains the conformation with the lowest energy, although the partial cone conformation with the anisole moiety rotated through the plane of the methylene groups is of comparable energy. The loss of one H bond in the partial cone conformation is compensated for by reduction of the electrostatic repulsion between the anisole oxygen and the other oxygens and the more favorable VDW energy of the partial cone conformation. For compound **1b** the dihedral angles in the calculated cone conformation are 73.5 (anisole), 45.5, 68.1, and 47.9° (phenols), showing that the deviations from a cone with C_{4v} symmetry are not so large, as was also deduced from its ^{1}H NMR spectrum.[31] The oxygen–oxygen distances are 2.73, 2.73, 2.88, and 2.98 Å. As there are three H bonds present in this conformation, this means that one H bond is weaker than the other two. This is probably the H bond to a methoxy oxygen atom, as this oxygen bears less negative charge than a hydroxyl oxygen atom.

For the dimethyl ether **1c** none of the conformations is clearly preferred in the calculations. The cone conformation is not anymore the only conformation in which all possible (in this case two) H bonds can be accommodated, and therefore, other conformations that have a more favorable VDW or bonded energy or have a lower electrostatic repulsion between the oxygen atoms become important. The 1,3-alternate conformation, in which no H bonds are possible, is even the conformation with the lowest energy, because of its low bonded and VDW energy and because of the small electrostatic repulsion between the oxygen atoms. ^{1}H NMR studies show that this compound is present in a cone conformation with C_{2v} symmetry in $CDCl_3$ solution.[29,31]

The crystal structure of the dimethyl ether **1c** was solved by X-ray crystallography and it shows the molecule to be present in a cone conformation with approximate C_{2v} symmetry (see Figure 2). The two anisole moieties are more or less parallel to each other, with the methoxy groups pointing outwards, while the two phenol units are flattened. This geometry can be rationalized in terms of reduction of the repulsion between especially the two oxygen atoms of the methoxy groups. The dihedral angles between the phenyl rings and the plane of the four methylene groups are 82.7 and 89.2° (calculated for the cone, 80.4°) for the anisole groups and 34.4 and 38.4° (calculated, 38.4°) for the phenol groups. The positions of the phenolic hydrogen atoms could not be determined from the collected reflection data. The asymmetry in the X-ray molecular structure, however, makes it possible to claim with reasonable certainty that H bonds are present between O1 and O2 and between O3 and O4. The distances between the two oxygens in both pairs are 2.82 and 3.00 Å (calculated, 2.90 Å), which are notably shorter than the distances between O1 and O4, 3.05 Å, and between O2 and O3, 3.11 Å (calculated, 3.09 Å for both). The hydrogen bonds in this dimethyl ether are weaker than in the parent calix[4]arene **1a**, as can be deduced from the longer oxygen–oxygen distances. This is confirmed by data from IR spectra. The OH-stretch vibrations change from 3150 cm^{-1} in **1a** to 3450 cm^{-1} in **1c**,[1,29] indicating that in **1c** the interaction of the hydroxyl hydrogen atom with other atoms is considerably reduced. The agreement between the calculated structure and the X-ray molecular structure is satisfying, although it must be noted that the experimental structure is more irregular than the calculated structure.

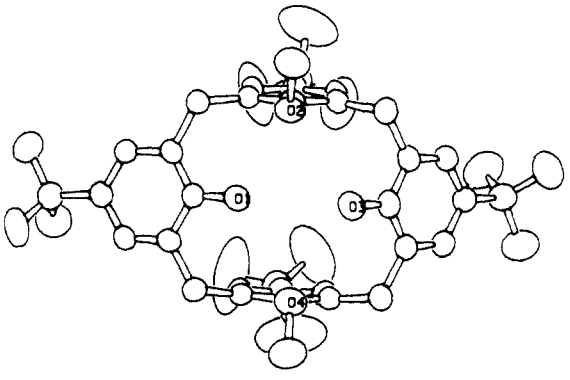

Figure 2. Crystal structure of **1c**, with the numbering of the oxygen atoms as used in the text. Hydrogen atoms are not shown.

Gutsche proposed that the two methoxy groups are pointing inwards, so that they shield the two hydroxyl groups from their surroundings, thus explaining why the dimethyl ether does not easily react further to the tri- and tetramethyl derivatives.[29] Calculations show that this conformation has an 11.2 kcal mol^{-1} higher energy than the cone conformation with the methoxy groups pointing outwards. This difference is mainly due to VDW repulsions between the methyl groups and unfavorable torsional energies. The inside conformation of both the methoxy groups seems therefore highly improbable.

There is a structural isomer of the 1,3-dimethyl ether **1c** possible, in which the hydroxyl groups of two neighboring phenyl units are replaced by methoxy groups. This compound, **1d**, has not been reported yet. The calculations predict for compound **1d** a partial cone conformation, in which an anisole unit is rotated through the plane of the methylene groups, to have the lowest energy. This energy is not only ~2.9 kcal mol^{-1} lower than the energy of the next conformation, the 1,3-alternate conformation, but is also 2.9 kcal mol^{-1} lower than the energy of the most stable conformation of the other dimethyl ether, **1c**. This means that compound **1d** is predicted to be more stable than **1c**. The reason that compound **1d** is not formed in the methylation reaction is probably from kinetic origin: the anion of the monomethyl ether that leads to the formation of **1c** is much more stable than the anion leading to **1d**, because of much more favorable electrostatic interactions (because of both H bonds and electrostatic repulsions). Efforts are directed toward synthesis of the 1,2-dimethyl ether **1d** via an indirect way in order to check the results of these calculations.

(30) Gutsche, C. D.; Bauer, L. J. *J. Am. Chem. Soc.* **1985**, *107*, 6052–6059.
(31) Alfieri, C.; Dradi, E.; Pochini, A.; Ungaro, R. *Gazz. Chim. It.* **1989**, *119*, 335–338.
(32) (a) Andreetti, G. D.; Ungaro, R.; Pochini, A. *J. Chem. Soc., Chem. Commun.* **1979**, 1005–1007. (b) Andreetti, G. D.; Pochini, A.; Ungaro, R. *J. Chem. Soc., Perkin Trans. 2* **1983**, 1773–1779. (c) Ungaro, R.; Pochini, A.; Andreetti, G. D.; Sangermano, V. *J. Chem. Soc., Perkin Trans. 2* **1984**, 1979–1985. (d) Ungaro, R.; Pochini, A.; Andreetti, G. D.; Domiani, P. *J. Chem. Soc., Perkin Trans. 2* **1985**, 197–201.

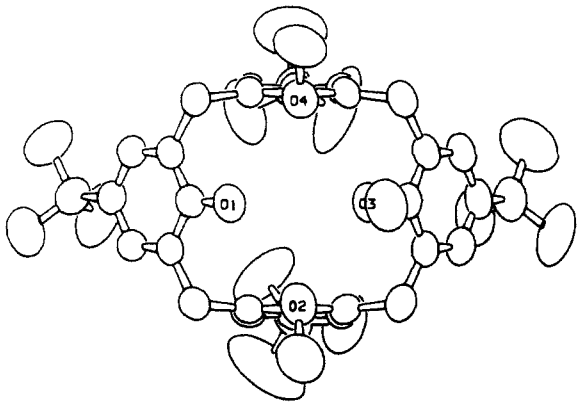

Figure 3. Crystal structure of **1e**, with the numbering of the oxygen atoms as used in the text. Hydrogen atoms are not shown.

For the trimethyl ether **1e** the calculations predict the 1,3-alternate conformation as the most stable conformation. Two partial cone conformations in which different anisole units are rotated through the plane of the methylene groups have a less than 1 kcal mol^{-1} higher energy. The ^{1}H NMR spectrum has been interpreted in terms of a cone conformation, in which both the phenol unit and the diametrical anisole unit are flattened and the other two anisole groups are nearly parallel to each other.[31] The calculated energy of this conformation is ~3.5 kcal mol^{-1} higher than that of the 1,3-alternate conformation, showing that the calculations fail to predict the right lowest energy conformation in this case.

The X-ray structure of compound **1e** shows an irregular cone conformation (see Figure 3). The dihedral angles of the phenyl rings with the mean plane of the methylene groups are 81.1, 45.7, and 87.4° (calculated for the cone, 82.4, 30.0, and 87.4°) for the anisole rings and 43.6° (36.2°) for the phenol ring. The acquired X-ray reflection data did not allow for the location of the phenolic hydrogen atom. Again, the position of this hydrogen atom can be predicted on the basis of the differences in the distances between neighboring oxygen atoms and comparison with the calculated structure. These distances are (those in parentheses are the calculated distances) as follows: O1···O2 = 2.96 (2.93) Å, O2···O3 = 3.00 (3.03) Å, O3···O4 = 3.03 (3.25) Å, and O4···O1 3.08 (3.41) Å. Consequently, the hydrogen atom is most likely located between O1 and O2. This hydrogen bond is again relatively weak. The agreement between the calculated and experimental geometry is reasonable. The most serious deviations stem from the flattened rings, which are more flattened in the calculated than in the experimental structure.

For the tetramethyl ether **1f** the calculations predict the 1,3-alternate conformation to be the most stable conformation, followed by the partial cone (the energy difference is ~1.8 kcal mol^{-1}). These two conformations are preferred by all energy contributions. In solution the partial cone conformation is the most stable conformation.[29] The X-ray structure shows that compound **1f** adopts a partial cone conformation in the solid state, in which all the methoxy groups point outwards (see Figure 4). The dihedral angles between the phenyl rings and the mean plane of the methylene groups are 88.3, −88.0, 84.8, and 35.3° (calculated for the partial cone, 88.3, −88.9, 89.9, and 25.2°). The agreement between the X-ray molecular structure and the calculated structure is reasonably good. The flattened phenyl ring is more flattened in the calculated structure than in the X-ray structure, as was found for the trimethyl ether. (The experimental values have been calculated for one of the two independent molecules. The values for the second molecule differ by no more than 2.2°.)

On the basis of an extra signal in the ^{1}H NMR spectrum of **1f**, Gutsche postulated that methoxy group 1 can be present in two positions, either pointing outwards or pointing inwards.[29] When it is in the "inside" position it partly fills the cavity of the molecule. Calculations on this last conformation gives an energy that is 5.0 kcal mol^{-1} higher than the energy of the outside conformation, which is a rather large difference. However, in the present calculations no account is taken of $CH_3\cdots\pi$ interactions. Recently, it was shown that these interactions might play a role in the complexation of neutral guests by calix[4]arenes.[33] The same interactions can also play a part in this self-complexation of a methoxy group in the cavity of calix[4]arene **1f**.

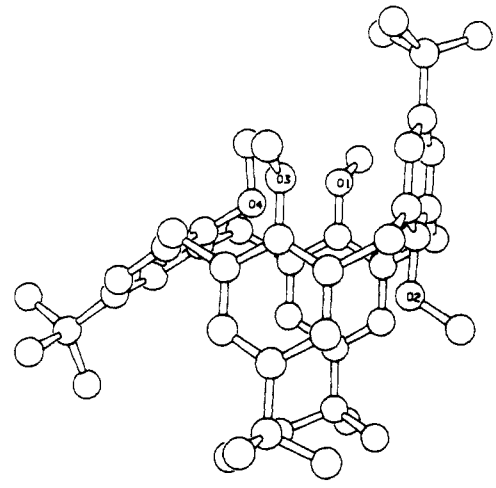

Figure 4. Crystal structure of **1f**, with the numbering of the oxygen atoms as used in the text. Only one of the two independent molecules in an asymmetric unit is shown. Hydrogen atoms are not shown.

Most of the tetrasubstituted calix[4]arenes that have been synthesized were isolated in the cone or in the partial cone conformation, and only a few in the 1,3-alternate conformation. Gutsche and Ungaro have shown that when the substituents are larger than a methoxy group, the conformation of the tetrasubstituted calix[4]arene is rigid.[29,34] The cone conformation of tetrasubstituted calix[4]arenes is normally deduced from its ^{1}H NMR spectrum, which shows signals that are commensurate with a cone with C_{4v} symmetry. However, X-ray structures of uncomplexed tetrasubstituted calix[4]arenes[35] and also our calculations on the cone conformation of **1f** show that the cone has actually only C_{2v} symmetry. The cone structure with C_{4v} symmetry is calculated to be a saddle-point structure with a 3.2 kcal mol^{-1} higher energy than the C_{2v} structure. That this is not reflected in the ^{1}H NMR spectrum is probably due to rapid interconversion of the two possible cone structures with C_{2v} symmetry.

The effects of the para substituent on the conformation of a calix[4]arene have also been investigated. Gutsche has shown that the conformations of unsubstituted calix[4]arene and of its tetramethyl ether do not change when the *tert*-butyl groups are removed.[29] Only the flexibility of the unsubstituted calix[4]arene is slightly dependent on the nature of the para substituent.[30] In recent work on selective functionalization of the upper rim of the calix[4]arenes,[36] the 1,3-dimethyl ether of calix[4]arene (**1g**) was synthesized, and its X-ray structure could be determined. This allows for comparison of both the X-ray molecular structures and the calculated structures of two calix[4]arenes with different para substituents. The X-ray molecular structure of compound **1g** is shown in Figure 5. The dihedral angles of the phenyl rings with the mean plane of the methylene groups are 78.3 and 75.5° (calculated, 77.6°) for the anisole rings and 43.9 and 37.0°

(33) Andreetti, G. D.; Ori, O.; Ugozzoli, F.; Alfieri, C.; Pochini, A.; Ungaro, R. *J. Inclusion Phenom.* **1988**, *6*, 523–536.
(34) Bocchi, V.; Foina, D.; Pochini, A.; Ungaro, R.; Andreetti, G. D. *Tetrahedron* **1982**, *38*, 373–378.
(35) (a) Ungaro, R.; Pochini, A.; Andreetti, G. D. *J. Inclusion Phenom.* **1984**, *2*, 199–206. (b) McKervey, M. A.; Seward, E. M.; Ferguson, G.; Ruhl, B.; Harris, S. J. *J. Chem. Soc., Chem. Commun.* **1985**, 388–390. (c) Arduini, A.; Pochini, A.; Reverberi, S.; Ungaro, R.; Andreetti, G. D.; Ugozzoli, F. *Tetrahedron* **1986**, *42*, 2089–2100. (d) Ferguson, G.; Kaitner, B.; McKervey, M. A.; Seward, E. M. *J. Chem. Soc., Chem. Commun.* **1987**, 584–585. (e) Calestani, G.; Ugozzoli, F.; Arduini, A.; Ghidini, E.; Ungaro, R. *J. Chem. Soc., Chem. Commun.* **1987**, 344–346.
(36) van Loon, J. D.; Arduini, A.; Verboom, W.; van Hummel, G. J.; Harkema, S.; Ungaro, R.; Reinhoudt, D. N. *Tetrahedron Lett.* **1989**, *30*, 2681–2684.

Table IV. Comparison of Several Force Fields and the AM1 Method for Calculations on Calixarene **1i**[a]

conformation	AMBER 3.0 all atom	MACROMODEL 1.5 AMBER all atom	MACROMODEL 1.5 MM2 all atom	MM2P(85)	QUANTA CHARMm 2.1A	AM1
cone	0	0	0	0	0	-40.4
partial cone	-5.1	-4.5	-1.8	-1.9	-2.5	-35.2
1,2-alternate	-5.1	+0.5	+0.8	+3.2	+6.0	-37.8
1,3-alternate	-9.3	-5.4	-1.9	-1.4	-1.0	-29.5

[a] For the molecular mechanical results total energies are given relative to the energies of the cone conformations; for the AM1 results the heat of formation is given; both in kcal mol^{-1}.

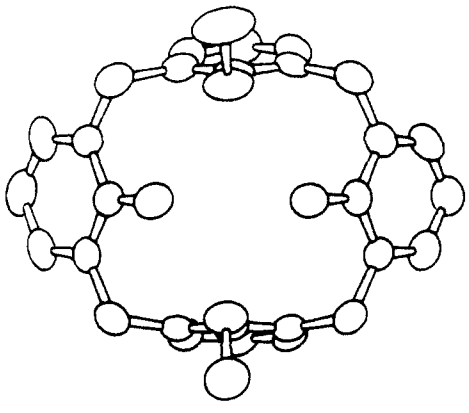

Figure 5. Crystal structure of **1g**. Only one of the two independent molecules in an asymmetric unit is shown. Hydrogen atoms are not shown.

(calculated, 37.5°) for the phenol rings. The oxygen–oxygen distances are 2.86, 2.93, 2.92, and 2.96 Å (calculated, 2.89 and 3.03 Å). (Experimental values have been calculated for one of the two independent molecules in an asymmetric unit.) There are small differences between the X-ray molecular structures of dimethyl ethers **1c** and **1g**. The phenol rings in **1c** are somewhat more flattened than in **1g**, and the two anisole units are more parallel to each other. This brings the para positions of the anisole rings in **1c** closer together. This same effect, although smaller, is found in the calculated structures. Comparison of the calculated energies of the conformations of compounds **1c** and **1g** shows that the preference of **1c** for the 1,3-alternate conformation changes to a preference for the cone conformation when the *tert*-butyl groups are removed (see Table III). For **1g**, the 1,3-alternate, and to a lesser extent the partial cone conformation, have a higher VDW energy relative to the other conformations than for **1c**. This means that part of the stabilization energy of the 1,3-alternate and the partial cone is due to favorable VDW interactions between the *tert*-butyl groups on the para positions.

The same trend is found when the energies of the different conformations of tetramethoxycalix[4]arenes with *tert*-butyl, methyl, and hydrogen on the para position are calculated. The order of the energies of the conformations does not change, but the energy of the 1,3-alternate conformation becomes relatively higher because of increasing VDW energies, going from *tert*-butyl via methyl to hydrogen. Also here, the involved energy effects are fairly small, but significant.

In order to investigate the influence of the force field used on the results of the calculations, we performed some calculations on the different conformations of the tetramethyl ether of *p*-methylcalix[4]arene **1i**. The results, summarized in Table IV, show that AMBER and the AMBER and MM2 force fields in MACROMODEL give the 1,3-alternate as the lowest energy conformation. Both the MM2P(85) and the QUANTA/CHARMm program calculate the partial cone to be the conformation with the lowest energy, which would be expected to be the most stable conformation, in analogy with the *p-tert*-butyl derivative **1f**. The energies of the four conformations were also minimized with the AM1 method. This leads to results that differ completely from the results of both experiments and MM calculations.

Dynamics of Conformational Interconversions in Calixarenes. Two pathways have been suggested for the cone-to-cone interconversion of calixarene **1h**: the "broken-chain"[37] and the "continuous-chain"[30] pathway. In the first one the 1,3-alternate conformation would be a key intermediate, while in the second one an activated complex resembling the 1,2-alternate conformation would be a key intermediate. In order to study conformational interconversions in calixarene **1h** we carried out molecular dynamics simulations on one isolated molecule **1h** at temperatures of 300, 600, and 800 K for 50 ps. Initially, we did not include solvent molecules in the calculations since the rate of the interconversion of the cone conformation is ca. 100 s^{-1} at 318 K in $CDCl_3$, meaning that on a time scale of 50–100 ps, which is characteristic for most MD calculations, not a single interconversion is likely to be observed at the temperatures under study. However, in the gas phase the rate of interconversion is drastically enhanced and our MD simulations show several conformational transitions within 50 ps at 300 K. We analyzed the trajectories in two ways, i.e., visually by inspecting MD movies on a graphics terminal, and computationally by monitoring the distance between averaged positions of the oxygen atoms on one hand and the methylene carbon atoms on the other hand, as a function of time (Figure 6). It turns out that this distance possesses characteristic values for the cone, partial cone, and alternate conformations.

Visual inspection of MD movies suggests that at 300 K the motions of the two phenol moieties opposite to each other are initially strongly coupled when the calixarene is in its cone conformation. Only after 35 ps does one of the phenol moieties break its hydrogen bonds with the other phenols and flip through the cavity, resulting in the partial cone conformation (see Figure 6a). The characteristic monitored distance (see above) for the cone, partial cone, and the 1,2- and 1,3-alternate conformations (the latter two fall in the same range) amount to approximately 1.2, 0.6, and 0.2 Å, respectively. After adopting the partial cone conformation for a few picoseconds the molecule starts interconverting between the 1,2- and 1,3-alternate conformations and the partial cone. At 600 K only one conformational interconversion is observed in the 50-ps trajectory. However, the amplitude of the coupled movements of the phenolic moieties are much larger at this temperature, resulting in larger fluctuations in the monitored distance (Figure 6b). At 800 K an almost continuous interconversion of the calixarene is observed (see Figure 6c). Three times (after 3, 18, and 37 ps) the cone conformation interconverts to another conformation, only once via the partial cone conformation. Given the relatively short trajectories it is hard to draw definitive conclusions. However, in a number of cases essentially the same interconversion pathway was observed, i.e., first one of the phenol moieties involved in the coupled movement flips through the cavity resulting in the partial cone conformation, and then a second one flips through and the 1,2-alternate or 1,3-alternate conformation is adopted. After this several transitions are observed in which all possible "noncone" conformations were formed before finally, again via a partial cone intermediate, the cone conformation was adopted by the calixarene. It is quite clear from the MD movies that the strongly coupled movement of the two pairs of opposite phenol moieties favors the conformational transitions. Although these are all gas-phase calculations, the pathway suggested here seems to be of relatively low energy and may have some relevance for the situation in an apolar solvent.

(37) Kämmerer, H.; Happel, G.; Caesar, F. *Makromol. Chem.* **1972**, *162*, 179–197.

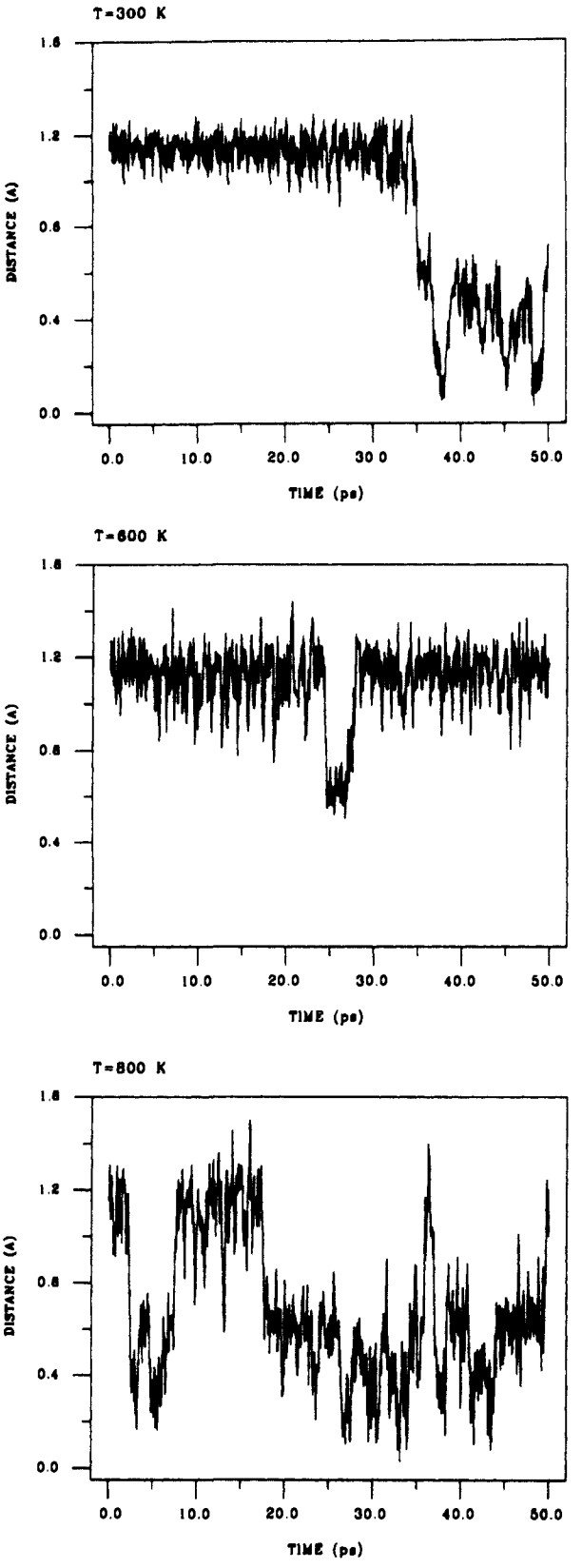

Figure 6. Distance between the averaged positions of the oxygen and methylene carbon atoms in **1h** as a function of the time at 300 K (a, top), 600 K (b, middle), and 800 K (c, bottom).

In order to study the possible role of solvent assistance for a *polar* solvent, we also carried out an MD simulation of **1h** in a droplet of 236 water molecules at 300 K. The MD trajectory was studied by applying the same methods as used for the gas-phase simulations. To our surprise we noticed that the calixarene started showing conformational transitions on the same time scale as was observed for the isolated molecule simulation at 300 K. After

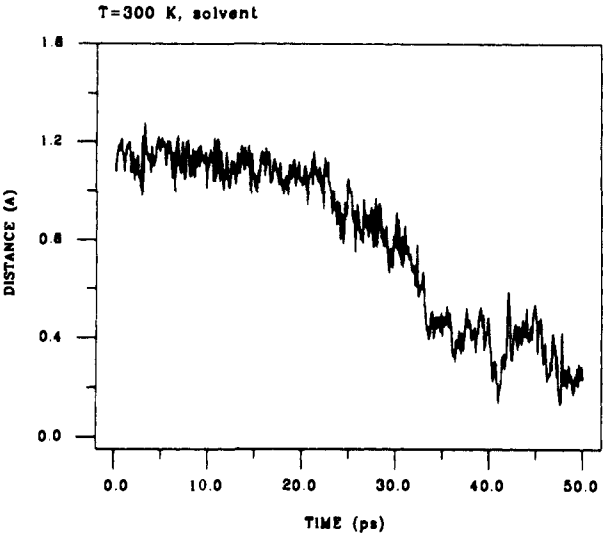

Figure 7. Distance between the averaged positions of the oxygen and methylene carbon atoms in solvated **1h** as a function of the time at 300 K.

~30 ps the conformation changed from the cone to the partial cone, and in almost continuous fashion to the 1,3-alternate conformation. It is clear that the conformational transitions proceed more smoothly for the solvated calixarene than for the gas-phase calixarene. This is easily seen by comparing the two plots showing the average characteristic distance in the gas phase (Figure 6a) and in the solvent (Figure 7).

A close look at the MD movie of the solvated calixarene reveals that the circular hydrogen-bonding scheme is less stable than in the gas phase, and water molecules act as hydrogen-bonding partners. Upon formation of the partial cone conformation, the phenolic moiety that rotates is initially hydrogen bonded to the opposite phenol oxygen atom, "pulling" it to a conformation that may be regarded as a precursor for the 1,3-alternate conformation. When the rotation of the phenolic moiety is complete and the partial cone conformation is adopted, this hydrogen bond is broken, and the phenolic group starts accepting a hydrogen bond from a water molecule. Meanwhile, the opposite phenol moiety, which has rotated partly, donates a hydrogen bond to another water molecule, located in the hydrophobic cavity. Within a few picoseconds the 1,3-alternate conformation is formed. Although the few conformational transitions observed in the solvent do not allow one to draw definitive conclusions, the simulations suggest that the activation barrier for the conformational transitions is lowered relative to the gas-phase situation by solvent assistence.

Flip–Flop Hydrogen Bonding. Special attention was directed to the possible presence of flip–flop hydrogen bonding in the calixarenes studied. In the three "gas-phase" MD simulations we found no occurrence of flip–flop hydrogen bonding by examining the 50-ps MD trajectories mentioned in the preceding section. Visual inspection of the MD trajectories pointed out that the O–H···OH hydrogen bonds stay directed to the same hydroxyl groups during the simulations. Only when conformational transitions are observed, are hydrogen bonds broken and formed, but in a noncoupled fashion.

The simulation of the solvated calixarene shows that the hydrogen-bonding scheme is definitely more dynamic than in the gas phase. Although the four hydroxyl oxygen atoms are the most important hydrogen bond acceptors for the neighboring or opposite hydroxyl groups (16–62% of the total "hydrogen-bonding time", depending on the phenol moiety), some water molecules also act as hydrogen bond acceptors. We studied the precise hydrogen-bonding scheme by analyzing every saved coordinate set, applying the same criteria for the occurrence of a hydrogen bond as was used in the cyclodextrin study,[6e] i.e., the OH···O distance must be smaller than 2.5 Å, and the O–H···O bond angle must be between 135 and 225°. Again, no flip–flop hydrogen bonding was observed on the time scale of the simulation (50 ps). The

Table V. Results (in kcal mol^{-1}) of Free Energy Perturbation Calculations on Calixarene **1h** and 2,4,6-Trimethylphenol **2a**

		ΔG_{pert}					ΔG_{total}				
compd	n	cone	partial cone	1,2-alternate	1,3-alternate	ΔG_{corr}	cone	partial cone	1,2-alternate	1,3-alternate
1h	0	−64.0	−64.4	−63.7	−61.2	−20.5	−84.5	−84.9	−84.2	−81.7
1h	1	−26.7	−27.8	−29.9	−29.5	−61.5	−88.2	−89.3	−91.4	−91.0
1h	2	8.9	7.7	5.2	5.0	−102.5	−93.6	−94.8	−97.3	−97.5
1h	3	44.0	45.0	44.0	41.1	−143.5	−99.5	−98.5	−99.5	−102.4
2a	0			−48.9		−20.5			−69.4	

Table VI. Results from the Semiempirical Calculations on Calixarene **1h** and Its Polyanions

total charge	heat of formation, kcal mol^{-1}	OH···O hydrogen bonding				arom C–CH_2–arom C av angle, deg
		no.	type	av distance, Å	av angle, deg	
0	−121.36	2	linear	2.070 ± 0.001	128.7 ± 0.2	111.6 ± 0.2
		2	linear	2.047 ± 0.004	167.8 ± 0.8	
−1	−160.82	2	linear	1.932 ± 0.000	162.2 ± 0.1	112.1 ± 0.5
		1	bifurcated	2.181 ± 0.003	125.2 ± 0.2	
−2	−124.43	2	bifurcated	2.194 ± 0.003	124.4 ± 0.3	112.7 ± 0.1
−3	−15.24	1	linear	2.039	154.7	114.0 ± 0.5
−4	144.29	na	na	na	na	114.0 ± 0.5

average hydrogen-bonding distance and angle between two hydroxyl groups amounted to 1.87 Å and 150°.

Relative Acidities of Calixarenes. In Table V, the results of the free energy perturbation studies are collected. During the perturbation studies the conformation of the calixarene did not change from its starting conformation, i.e., cone remained cone, partial cone remained partial cone, etc. The simulations were carried out for all four conformations. Recent NMR studies in DMSO by Gutsche et al. suggest that the mono- and tetraanions are in the cone conformations but the trianion would adopt a partial cone conformation.[38] We used three different models for the perturbing group.[21] The smallest perturbing group was made up of three atoms, i.e., the O and H atoms of the hydroxyl group and the ipso carbon atom. The medium-sized group consisted of the whole phenolic moiety and the largest perturbing group model consisted of the phenolic moiety with the two methylene groups at the 2- and 6-positions. Since it turned out that the size of the group did not significantly change the magnitude of the relative free energies, we will discuss the results of the medium-sized group only.

Perturbing the first phenolic moiety of **1h** to a phenolate anion is thermodynamically very unfavorable, the total free energy amounting to values between −81.7 and −84.9 kcal mol^{-1}, depending of the conformation of the calixarene. The reason for this very favorable process is of course the drastically enhanced electrostatic interactions between solvent and (negatively charged) solute. In addition, the intramolecular hydrogen bonding in the calixarene is increased as semiempirical studies indicate (vide infra). Therefore, the least favorable deprotonation is predicted to take place for the 1,3-alternate conformation, in which the stabilizing effect of hydrogen bonding is limited due to the relative large distances between the hydroxyl groups. This is nicely confirmed by our calculations.

The ΔG_{pert} for the second, third, and fourth deprotonation gradually becomes more and more favorable due to the increasing repulsive interactions between the negatively charged phenolate moieties. However, after the reaction field correction is made, the ΔG_{total} is predicted to become more and more favorable, in contrast with chemical intuition and experiment.[7,39] It must be noted that the magnitude of the reaction field correction ΔG_{corr} is becoming increasingly larger relative to ΔG_{pert} and is certainly the least accurate quantity in the calculation of ΔG_{total}. It is clear that the calculations for the multideprotonated calixarenes do not allow us to draw decisive conclusions about the preferred conformations of the polyanionic species. However, the calculated free energies of deprotonation do not seem to be very much dependent on the conformation. The differences in the free energies for a given deprotonation step are all within 4 kcal mol^{-1}. Apparently for the first two deprotonations the overall free energies are dominated by solute–solvent interactions, whereas for the last two deprotonations the intramolecular repulsive interactions play the most important role. Therefore, differences in the hydrogen-bonding scheme around the anionic oxygen atoms for the various conformations seem to be less important. This was confirmed by the following analysis. When the monoanion is perturbed into the dianion (n = 1) for the cone conformation, there are two positions for the perturbing group relative to the anionic phenol moiety. The ΔG_{pert} for neighboring versus opposite positions are −30.1 ± 3.4 and −26.7 ± 2.2 kcal mol^{-1}, respectively, showing that the effect of the position in the macrocycle is relatively small.

When the perturbation is carried out for the open-chain model **2a**, the total free energy of −69.4 kcal mol^{-1} is less favorable than for the corresponding perturbation of **1h**. The difference in free energies falls in the range 12.3–15.5 kcal mol^{-1} which is equivalent to a difference of 9–11 pK_a units. This is in the same order as the difference in pK_a for a calixarene with R = NO_2 and 4-nitrophenol, being more than 7 pK_a units in H_2O[7] and 6.2 pK_a units in 85.4 wt % EtOH/H_2O.[39] It is clear that the higher acidity of **1h** relative to **2a** is caused by the presence of "preorganized" hydrogen-bonding donors in the calixarene itself. Although water molecules can form hydrogen bonds to the negatively charged oxygen atoms as well, the entropy price for the reorientation and proper alignment is much higher for the water molecules. In the calixarene the entropy price has been paid during the synthesis.[40] This explanation is consistent with the results from Monte Carlo studies of the hydration of ions by Jorgensen et al.,[41] who have shown that the orientation of the first solvation shells causes a significant loss in the solvent–solvent attraction.

Structural and Energetical Features of (Poly)anionic 1h and 2a. In order to determine the amount of charge delocalization and hydrogen bonding in the calixarene (poly)anions in the cone conformation, semiempirical calculations were carried out using AM1. Although it is known that AM1 tends to underestimate the energy involved with hydrogen bonding, the calculation of geometries would not be affected seriously by this weakness.[16,42]

(38) Gutsche, C. D.; Iqbal, M.; Nam, K. S.; Alam, I. *Pure Appl. Chem.* **1988**, *60*, 483–488.

(39) The pK_a's for *p*-nitrocalix[4]arene were determined in 85.4 wt % EtOH/H_2O at 25 °C by potentiometric titration using tetrabutylammonium hydroxide: pK_{a1} 2.9, pK_{a2} 10.9, pK_{a3} 12.3, and pK_{a4} > 13. The pK_a of *p*-nitrophenol is 8.67 in this same solvent. Grootenhuis, P. D. J.; Reinhoudt, D. N.; Shinkai, S., unpublished results.

(40) See for further discussions on the effects of preorganization: Kollman, P. A.; Wipff, G.; Singh, U. C. *J. Am. Chem. Soc.* **1985**, *107*, 2212–2219.

(41) Chandrasekhar, J.; Spellmeyer, D. C.; Jorgensen, W. L. *J. Am. Chem. Soc.* **1984**, *106*, 903–910.

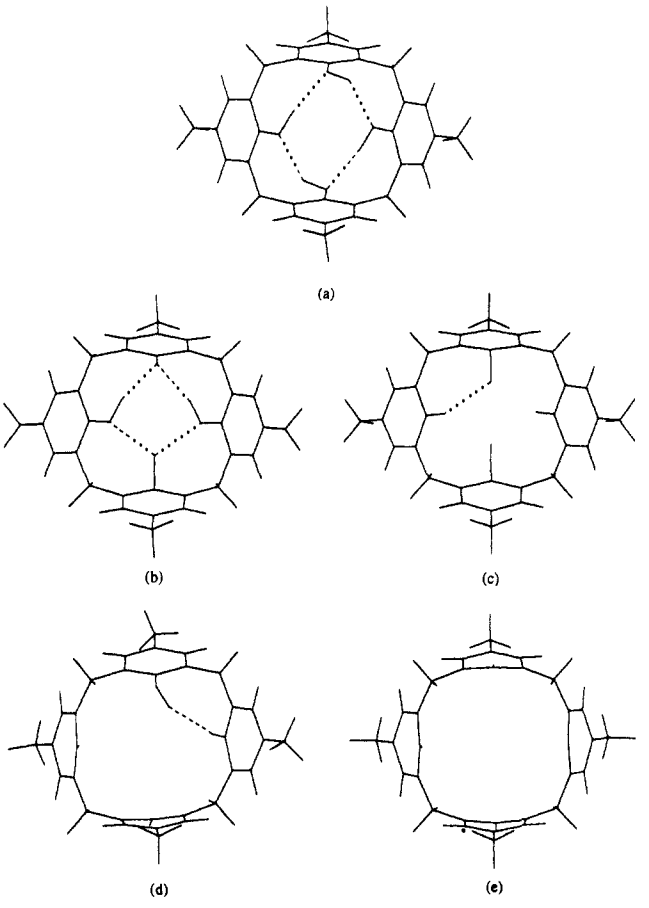

Figure 8. AM1-optimized structures of neutral (a), monoanionic (b), dianionic (c), trianionic (d), and tetraanionic (e) **1h**.

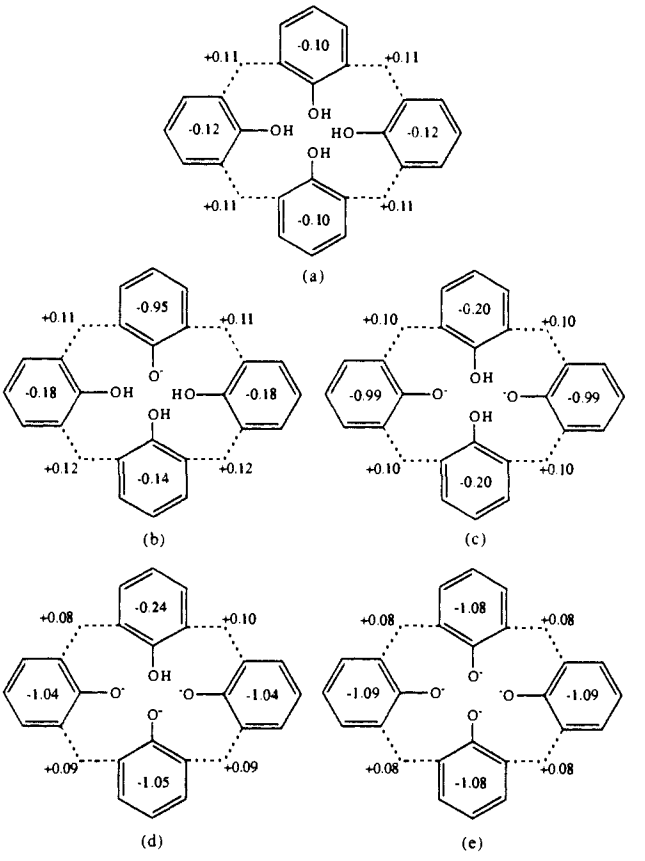

Figure 9. Charge delocalization calculated by AM1 in neutral (a), monoanionic (b), dianionic (c), trianionic (d), and tetraanionic (e) **1h**.

The results are summarized in Table VI and Figures 8 and 9.

The hydrogen bonding in neutral **1h** is nonsymmetric and consists of two short, almost linear hydrogen bonds together with two longer hydrogen bonds with rather unfavorable bond angles of 128.7°. Upon the first deprotonation two very short 1.93-Å hydrogen bonds are formed between the phenolate oxygen and the neighboring hydroxyl groups. In addition, a bifurcated hydrogen bond is formed (see Figure 8). Apparently, the combination of increased hydrogen bonding and charge relocalization in the monoanion amounts to almost 40 kcal mol^{-1}. In order to determine the hydrogen-bonding component we also calculated the heats of formation of **2a** and its anion, which are −43.59 and −63.73 kcal mol^{-1}, respectively. Since in the acyclic molecule no hydrogen bonding can occur, the 20 kcal mol^{-1} difference is due to charge delocalization only. Therefore, the difference in hydrogen bonding between neutral and monoanionic **1h** is estimated to be 40 − 20 = 20 kcal mol^{-1}. While one would expect a further increase in the hydrogen-bonding energy after the second deprotonation, AM1 indicates that only two relatively weak bifurcated hydrogen bonds are left, and the heat of formation increases with 36 kcal mol^{-1}. It is unclear if this result originates from the earlier mentioned weakness of AM1 in calculating hydrogen bond energies or if there really is a serious disruption of the hydrogen-bonding scheme of the dianionic species. In the trianionic species there is only one hydrogen bond. The large electrostatic repulsion between the oxygen atoms results in a heat of formation that is 106 kcal mol^{-1} higher than the neutral species. The tetraanionic species has a heat of formation that is 265 kcal mol^{-1} higher than **2a**. In this case the repulsive interactions force the oxygen atoms as well as the ipso carbon atoms to bend out of the aromatic plane. The average angle between the ipso and ortho carbons amounts to 114.0°. Another indication for the increasing steric strain in the macrocycle upon deprotonation is the increasing bond angle between the ortho carbon atoms and the methylene carbons.

The charge delocalization in the (poly)anions is depicted in Figure 9, where the sum of partial atomic charges is divided into "aromatic" and "aliphatic" portions.

Upon deprotonation the charge delocalization increases, as can be concluded from the decreased charges of the methylene groups and the protonated phenolic moieties. It is unclear if AM1 performs well with respect to the charges in these highly charged systems, but given the size of the molecules, this method is the only computationally feasible possibility at this moment. Generally, the amount of charge delocalization is not very large at this level.

Discussion

Conformational Analysis of Substituted Calix[4]arenes. The MM calculations using the AMBER force field (in MACROMODEL) give only in a few cases a lowest energy conformation that is the same as the experimentally found conformation. For calixarenes **1c**, **1e**, and **1f** a 1,3-alternate has a lower energy than the experimentally found conformations, which are the cone, the cone, and the partial cone, respectively. It is not easy to understand why the 1,3-alternate conformation is so much preferred in these calculations. Looking in detail at the components of the energies of the conformations of **1a–f** reveals that both the bonded energies and the van der Waals energies favor in all cases the 1,3-alternate conformation over the partial cone, the cone, and the 1,2-alternate conformation. The final conformation of a calix[4]arene is determined by the balance between these bonded and VDW energies at one side and the electrostatic and hydrogen bond energies at the other side. For molecules **1a** and **1b** the electrostatic energy associated with the H bonds in the cone conformation is so large that this energy overrules all other energy components, and indeed, the cone conformation is the experimentally observed conformation. For the other calixarenes the situation is not so clear. In the electrostatic component the favorable H-bond energies are more and more compensated by electrostatic repulsions between the (methylated) oxygen atoms. The electrostatic energy dif-

(42) Gilliom, R. D. *J. Chem. Educ.* **1989**, *66*, 47–50.

ferences between the different conformations are more or less equal to the differences in the bonded plus van der Waals energies, leading to partial cancellation of these energy differences. Unfortunately, this leads for all compounds to a wrong conformation having the lowest energy, i.e., wrong in comparison with the experimental data.

In order to check whether these results are reliable, we tried different force fields for calculations on a model compound, **1i**. These calculations showed that there exist pronounced differences between the different force fields. Two of them, MM2P(85) and QUANTA/CHARMm, calculate the partial cone conformation to have the lowest energy, the others the 1,3-alternate. Checking the energy components of these calculations revealed some interesting facts. All force fields give remarkably similar differences in the sums of the bonded and VDW energies for the four different conformations, leading to the order 1,3-alternate ≈ partial cone < cone < 1,2-alternate. Only AMBER 3.0 differs in that it calculates a much lower energy for the 1,3-alternate conformation. The differences in electrostatic energies on the other hand show large variations. Assuming that the experimentally found partial cone conformation for **1f** is also the conformation with the lowest energy for **1i**, it is clear that in the calculations with both MACROMODEL and AMBER 3.0 the electrostatic energy is calculated wrongly. MM2P(85) and QUANTA/CHARMm seem in this specific case more reliable.

With this last result and the fact that the relative energies of the conformations of calix[4]arene do not change much on going from a para methyl to a para *tert*-butyl substituent, we can conclude that for calixarenes **1a**, **1b**, and **1c** the cone conformation is the most stable conformation because of favorable electrostatic (hydrogen-bonding) interactions. For **1f**, the partial cone is the most stable, now because of relative low electrostatic repulsions between the oxygen atoms. For **1e** the observed preference for the cone conformation cannot be explained with the current results.

It should not be forgotten that MM calculations relate to isolated molecules, whereas the ^{1}H NMR and X-ray experiments with which the results are compared give information on molecules in solution and in the solid state. Specific intermolecular interactions between a molecule and the solvent or between molecules themselves can alter the relative stabilities of the different conformations of a molecule and also the geometry of a *hydrated* conformation of a molecule. And although the results of the present calculations are in reasonable agreement with experimental findings (for both relative energies and geometries of conformations) and most discrepancies can be explained without having to resolve to intermolecular interactions for possible explanations, it is still likely that intermolecular interactions do have influence on the observed conformations and their geometries. This might also be the case for **1e**.

Solvent Effects. The evaluation of solvent effects on the relative stabilities of calix[4]arene conformations and the role of solvation in conformational transitions is limited to a comparison of the simulations on isolated and *hydrated* species. Unfortunately, AMBER version 3.0 does not allow us to routinely perform the MD simulations using other solvents than water, so that a direct comparison with most experimental data is not possible. The MD studies on the conformational transitions indicate that the capability of water molecules to act as hydrogen-bonding partners has a considerable effect on the transitions. Because the water molecules are able to (partly) compensate the loss of OH···OH hydrogen bonds upon the conformational transitions, the process is more concerted-like. Therefore, the activation barrier of the interconversion seems to be lower, and at 300 K, the first transition was observed after a shorter time for the hydrated than for the isolated calixarene. Interestingly, in both simulations the partial cone conformation was the first conformation formed.

Free Energy Calculations. We find the agreement between the predicted and experimental differences in acidity between the calixarenes and their acyclic model compounds, very encouraging. However, the predicted trend that the dissociation into ions of the calixarenes becomes more and more easy does not make any chemical sense. There are several explanations why the results for creating multianionic species using the method described in this paper needs further correction. First, it is likely that the correction for the reaction field based on the Born formula (eq 4) is less reliable as the charges increase. Furthermore, the errors in applying it to a nonspherical model are unknown. Since this correction clearly dominates the total free energy at multiple negative charges, errors in this contribution will weigh heavily in the calculation of the total free energy. Second, the approximation that the bond dissociation energy for breaking the O–H bond for the di-, tri-, and tetraanions is the same, is probably not valid. The polarization of charges in the polyanionic species may be responsible for differences in this dissociation energy and such effects could make breaking successive O–H bonds more energetically costly. Correcting for such effects would tend to make ΔG_{pert} even more unfavorable for the highly charged anions and bring the results into qualitative agreement with experiment.

Although the results from similar FEP calculations on the successive protonations of tricyclic cryptand SC-24 showed a qualitative agreement with experimental data,[43] it is clear that at this point our model turns out to be too simple for making reliable predictions for relative pK_a differences in highly charged molecules. More reliable results would be obtained by the inclusion of polarization in the calculations of the electrostatic interactions (which is not possible in AMBER 3.0) and the improvement of the solvation model by evaluating more explicit solvent molecules, thus reducing the contribution of the reaction field correction. Both approaches will be the subject of future investigations.

Conclusions

In this study a wide range of properties of calix[4]arenes was assessed by computational methods. In general, good agreement was achieved between theory and available experimental data. In the cases where discrepancies between theory and experiment were found, satisfactory explanations for the failures could be given and follow-up calculations could be suggested. Some predictions were made concerning the pathways for conformational interconversion and the acidity of **1h**. With the exception of the ab initio calculations that were carried out in order to get the point charges for some molecular fragments, all the calculations were done on medium-sized computers that are expected to become more and more available to experimental chemists working in host–guest chemistry. We hope that the computational procedures and "experiments" described in this paper will further stimulate the use of computational tools in host–guest chemistry.

Acknowledgment. P.D.J.G. has been supported by a NATO Science Fellowship under the auspices of the Netherlands Organization for Scientific Research (NWO). P.A.K. is pleased to acknowledge research support from the Institute of General Medical Sciences (GM-29072). L.C.G. is supported by the Netherlands Foundation for Chemical Research (SON) with financial aid from the Netherlands Organization for Scientific Research (NWO). We wish to acknowledge the use of the UCSF Computer Graphics Laboratory facilities supported by Grant RR-1081 to R. Langridge. We are pleased to acknowledge grants for computer time on the CRAY-XMP from the San Diego Supercomputer Center (SDSC) for carrying out some of the ab initio calculations. We gratefully acknowledge the CAOS/CAMM center in Nijmegen (NL), supported by SON (NWO), for use of the programs MACROMODEL and MM2P(85) on their VAX 11/785 computer.

Registry No. 1a, 60705-62-6; **1b**, 126186-30-9; **1c**, 122406-45-5; **1d**, 126109-82-8; **1e**, 126186-31-0; **1f**, 105880-81-7; **1g**, 125065-61-4; **1h**, 53255-02-0; **1i**, 126083-73-6; **2a**, 527-60-6.

Supplementary Material Available: Tables of atomic positional and thermal parameters, bond distances, and bond and torsional angles of the X-ray structures of compounds **1c**, **1e**, **1f**, and **1g** (30 pages). Ordering information is given on any current masthead page.

(43) Grootenhuis, P. D. J.; Malliavin, T.; Kollman, P. A., to be published.